Journal of Bioenergetics and Biomembranes, Vol. 31, No. 3, 1999

Structure and Function of the Bacterial bc_1 Complex: Domain Movement, Subunit Interactions, and Emerging Rationale Engineering Attempts

Elisabeth Darrouzet,[1] Maria Valkova-Valchanova,[1] Tomoko Ohnishi,[2] and Fevzi Daldal[1,3]

Received March 31, 1999

The ubiquinol: cytochrome *c* oxidoreductase, or the bc_1 complex, is a key component of both respiratory and photosynthetic electron transfer and contributes to the formation of an electrochemical gradient necessary for ATP synthesis. Numerous bacteria harbor a bc_1 complex comprised of three redox-active subunits, which bear two *b*-type hemes, one *c*-type heme, and one [2Fe–2S] cluster as prosthetic groups. Photosynthetic bacteria like *Rhodobacter* species provide powerful models for studying the function and structure of this enzyme and are being widely used. In recent years, extensive use of spontaneous and site-directed mutants and their revertants, new inhibitors, discovery of natural variants of this enzyme in various species, and engineering of novel bc_1 complexes in species amenable to genetic manipulations have provided us with a wealth of information on the mechanism of function, nature of subunit interactions, and assembly of this important enzyme. The recent resolution of the structure of various mitochondrial bc_1 complexes in different crystallographic forms has consolidated previous findings, added atomic-scale precision to our knowledge, and raised new issues, such as the possible movement of the Rieske Fe–S protein subunit during Q_o site catalysis. Here, studies performed during the last few years using bacterial bc_1 complexes are reviewed briefly and ongoing investigations and future challenges of this exciting field are mentioned.

KEY WORDS: Cytochrome bc_1 complex; complex III; facultative phototrophic bacteria; *b*- and *c*-type hemes; [2Fe–2S] cluster; membrane protein assembly, biogenesis.

INTRODUCTION

The ubiquinol:cytochrome *c* oxidoreductase, or the bc_1 complex, is a key component of mitochondrial and bacterial respiratory chains (Knaff, 1993; Gennis *et al.*, 1993; Brandt and Trumpower, 1994; Gray and Daldal, 1995). The bc_1 complex and its homolog the b_6f complex also play a central role in photosynthetic electron transfer in phototrophic bacteria, algae, and higher plants (Cramer *et al.*, 1996) and are members of a rapidly growing superfamily of cytochrome *bc* complexes. These membrane enzymes catalyze transfer of two electrons from their substrate hydroquinone (QH_2) to a one-electron acceptor [cytochrome *c* or plastocyanin] concomitantly with the generation of an electrochemical gradient across the membrane. Their structurally simplest forms are encountered in bacteria and are formed of a cyt *b* subunit with two *b*-type hemes (b_L and b_H), a cyt c_1 subunit with a *c*-type heme, and a high-potential [2Fe–2S] cluster containing a Fe–S subunit. These subunits form two catalytic domains, called Q_o and Q_i sites, located on each side of the membrane. It is generally accepted that the bc_1 complexes function

[1] Department of Biology, Plant Science Institute, University of Pennsylvania, Philadelphia, Pennsylvania 19104.
[2] Department of Biochemistry and Biophysics, Johnson Foundation, University of Pennsylvania, Philadelphia, Pennsylvania 19104.
[3] Author to whom correspondence should be addressed. Email: fdaldal@sas.upenn.edu.

0145-479X/99/0600-0275$16.00/0

via the modified Q-cycle mechanism (Mitchell, 1976; Crofts *et al.*, 1983; Brandt and Trumpower, 1994), and a crucial tenet of this mechanism of function is the bifurcation of electrons at the Q_o site during QH_2 oxidation. According to this scheme, one of the two electrons is transferred to the high-potential redox chain ([2Fe–2S] cluster and then cyt c_1) and the other to the low-potential redox chain (hemes b_L, b_H, and then $Q/Q^{\bullet -}$ at the Q_i site).

Bacterial bc_1 complexes, in particular those from the facultative phototrophs of *Rhodobacter* species, constitute attractive model systems for studying the catalytic core of the more elaborate mitochondrial complexes. They are structurally simpler and readily amenable to multidisciplinary studies extending from molecular genetics to spectroscopy. In the latter species, the presence of multiple respiratory pathways, such as the quinol oxidase branch independent of the bc_1 complex, allows respiratory growth of bc_1-deficient mutants, which are photosynthesis-deficient (Ps^-) (Daldal *et al.*, 1987). Moreover, these species yield inside-out vesicles (chromatophores) able to perform light-induced cyclic electron transfer between the photochemical reaction centers and the bc_1 complexes *in vitro* and provide an unequaled experimental system for analysis at a fast time scale of various reaction steps internal to the bc_1 complex.

The structural subunits of bacterial bc_1 complexes are usually encoded by an operon called *pet*ABC (or *fbc*FBC). Chromosomal deletions lacking *pet*ABC, plasmids carrying the genes complementing them *in trans*, and constructs overproducing the bc_1 complex are available in *Rhodobacter* species (see Gray and Daldal, 1995). These genetic systems have been used extensively to study spontaneous mutants resistant to bc_1 inhibitors as well as site-directed mutants and their revertants, and have prove to be extremely informative (for a partial list of available bc_1 complex mutants, see Brasseur *et al.*, 1996). In previous years, combined genetic and biochemical approaches have defined the location of the Q_o and Q_i domains on cyt *b* and suggested the presence of two partially overlapping subsites (Q_oI and Q_oII) for binding of stigmatellin and myxothiazol, which are potent inhibitors of QH_2 oxidation by the bc_1 complex (Gray and Daldal, 1995). These studies have also revealed the nature of the amino acid residues liganding the prosthetic groups (Yun *et al.*, 1991; Gray *et al.*, 1992; Davidson *et al.*, 1992a; Van Doren *et al.*, 1993a) and attributed specific structural or functional roles to various residues of the bc_1 complex (Atta-Asafo-Adjei and Daldal, 1991; Ding *et al.*, 1995a; Hacker *et al.*, 1993, 1994; Gray *et. al.*, 1994; Saribas *et al.*, 1995).

The first three-dimensional (3-D) structure of the mitochondrial bc_1 complex was reported 2 years ago (Xia *et al.*, 1997) and, since that time, additional and often more informative crystallographic structures for this enzyme have become available (Zhang *et al.*, 1998; Kim *et al.*, 1998; Iwata *et al.*, 1998). These structures of the bc_1 complex have directly consolidated many of the earlier, often indirectly inferred, findings mentioned above. More importantly, they also added atomic-scale precision to our knowledge about its structural details and raised new issues about its mechanism of function. In the first crystal structure of the mitochondrial bc_1 complex (Xia *et al.*, 1997), the distance of 31 A calculated between the [2Fe–2S] cluster of the Fe–S protein subunit and heme c_1 was paradoxically far too large to support the fast electron-transfer rate observed between these two cofactors (see, for example, Ding *et al.*, 1995a). Since then, more recent 3-D structures obtained in presence or absence of various inhibitors revealed different positions for the Fe–S protein subunit within the bc_1 complex (Zhang *et al.*, 1998; Iwata *et al.*, 1998; Kim *et al.*, 1998) (Table I and Fig. 1). It appears that none of these positions fits completely with the entire catalytic mechanism of the bc_1 complex, which involves transfer of the two electrons emanating from the oxidation of QH_2 separately to the [2Fe–2S] cluster and to the heme b_L. Hence, the idea that the head domain of the Fe–S protein subunit may move during Q_o site catalysis has emerged as an attractive hypothesis to rationalize the bifurcated electron transfer process.

In this review, recent studies performed using bacterial bc_1 complexes on the mechanism of function of the catalytic sites, the role of the ligands in controlling the properties of the cofactors, the nature of the dynamic subunit interactions, at the Q_o site in particular, and the factors governing the assembly of the subunits into a mature complex are summarized briefly. In addition, emerging approaches aimed at defining the structural elements responsible for the functional differences observed among the various *bc* complexes are also described.

CYTOCHROME c_1 SUBUNIT

The cyt c_1 subunit is anchored to the membrane by a C-terminal transmembrane helix (Konishi *et al.*, 1991) and is, so far, the least studied catalytic subunit.

Table I. Summary of the Crystallographic Data Illustrating the Different Positions of the Head Domain of the Fe–S Protein Subunit in Various Crystal Forms of Mitochondrial bc_1 Complex

Organism	Crystal form	Inhibitor[a]	Resolution (A)	Distance from [2Fe–2S] to (A)		Occupancy[b]		Displacement[c]		References
				b_L	c_1	c_1 position	b position	Rotation (8)	Translation (A)	
Bovine	$I4_122$	—	2.9	27	31		0.46	*		Xia *et al.*, 1997; Kim *et al.*, 1998
Bovine	$I4_122$	Stig					1.18	4.2*	1.1*	Kim *et al.*, 1998
Bovine	$I4_122$	MOA				0.53		134.2*	15.1*	Kim *et al.*, 1998
Chicken	$P2_12_12_1$	—	3	34	21	0.54	0.01	#		Zhang *et al.*, 1998
Chicken	$P2_12_12_1$	Stig		26	31	0	0.93	57#	16#	Zhang *et al.*, 1998
Chicken	$P2_12_12_1$	MOA	3			0.53	0			
Chicken	$P2_12_12_1$	no Q	3			0.65	0.01			
Bovine	$P6_522$	—		35	16			§		Zhang *et al.*, 1998; Iwata *et al.*, 1998
Bovine	$P6_522$	Stig						65§	21.2§	Zhang *et al.*, 1998;
Bovine	$P6_5$	—	2.8	31	27					Iwata *et al.*, 1998

[a] Inhibitor: — indicates the native structure; Stig and MOA correspond to the structures obtained in presence of stigmatellin and methoxyacrylstilbene, respectively; no Q refers to the structure obtained using a bc_1 complex depleted from ubiquinone.

[b] Occupancy refers to the peak height of electronic density of the iron atom of the [2Fe–2S] cluster normalized to the intensity of the peak for the iron atom of hemes *b*. c_1 and *b* positions refer to the two extreme positions encountered for the [2Fe–2S] cluster.

[c] Displacement refers to the different positions of the head domain of the Fe–S protein subunit in different structures. The rotation angle (8) and the distance (A) between the different position of the [2Fe–2S] cluster are given in reference to the native structure and the structures to be compared are indicated with the same symbol *, #, or §.

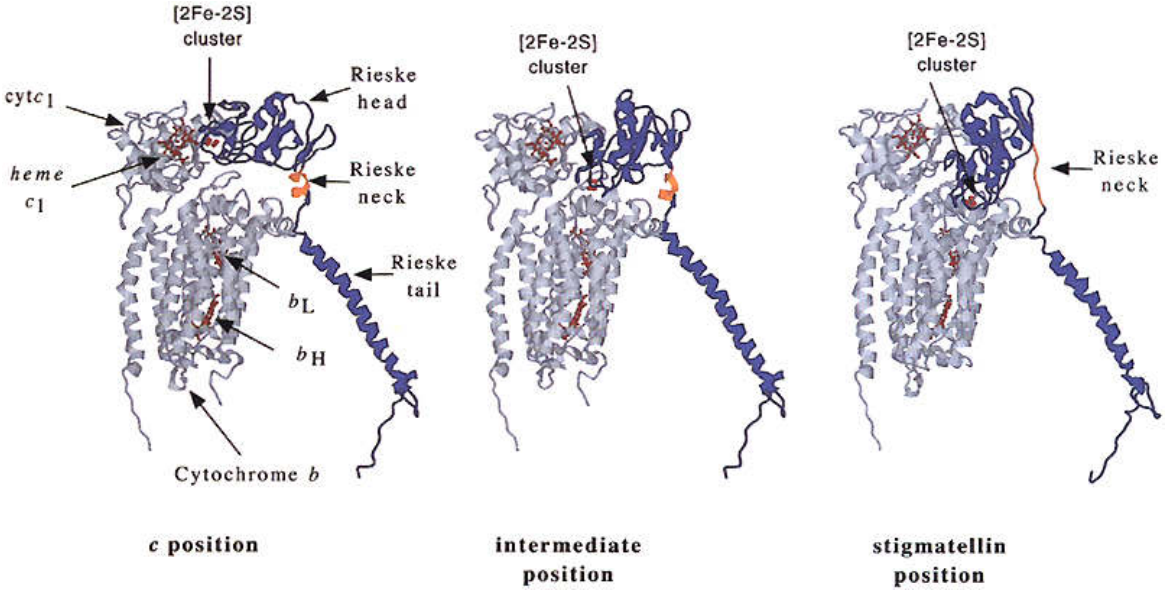

Fig. 1. Different positions of the Rieske Fe–S protein head domain. The structures of the three catalytic subunits of the bovine heart bc_1 complex in two different crystal forms in which the Rieske Fe–S protein head domain occupies two distinct positions ($P6_522$: cyt *c* position; $P6_5$: intermediate position) (Iwata *et al.*, 1998) and that of the chicken heart bc_1 complex in presence of stigmatellin (Zhang *et al.*, 1998) are shown. The Fe–S protein subunit is shown in blue with its flexible neck region encompassing the amino acid residues 67–73 (corresponding to 43–49 in *R. capsulatus*) in orange. Cyt *b* and cyt c_1 subunits are in gray and the cofactors (hemes b_L and b_H, heme c_1, and the [2Fe–2S] cluster) in red.

Like many *c*-type cytochromes, it contains a conserved CxyCH motif involved in covalent attachment of its heme group and a methionine (M) residue as the sixth axial ligand to its heme iron atom, as strongly inferred by many spectroscopic data (Simpkin *et al.*, 1989; Lou *et al.*, 1993; Finnegan *et al.*, 1996). Mutagenesis studies of the highly conserved methionine residues located near the C-terminal end of cyt c_1 has revealed that in *R. capsulatus*, M183 is indeed the sixth axial ligand (Gray *et al.*, 1992). Crystallographic data for the mitochondrial bc_1 complex has confirmed this assignment (Xia *et al.*, 1997; Zhang *et al.*, 1998; Iwata *et al.*, 1998), whereas in chloroplast b_6f complex, the sixth axial ligand of cyt *f* is provided by the free amino group of the N-terminal tyrosine residue (Martinez *et al.*, 1994). In *R. capsulatus*, mutagenic substitution of M183 by a nonliganding residue like a leucine (L) nicely evidenced the critical role of the sixth ligand in setting the E_m value of cyt c_1 (Gray *et al.*, 1992). This study also revealed that a subpopulation of M183L cyt c_1 mutant exhibits spectroscopic properties characteristic of a hexacoordinated heme, possibly via a bis-histidine (H) ligation (Gao *et al.*, 1999). Additional studies indicated that partial unfolding, enhanced upon exposure to cryoprotectants, can produce similar spectra even with the wild-type cyt c_1 (Finnegan *et al.*, 1996). These findings stimulated further investigations on the role played by the sixth axial ligand in heme–protein interactions by engineering of novel cyt c_1 variants with possible histidine–lysine (K) and histidine–histidine axial coordinations (Darrouzet *et al.*, 1999) (Fig. 2). Characterizations of these mutants revealed that they incorporated the heme group into their cognate cyt c_1 polypeptides and assembled the mature subunits into nonfunctional bc_1 complexes. Mutants cyt c_1 had unusual spectroscopic and thermodynamic properties, such as shifted optical absorption maxima (λ_{max}) and highly decreased E_{m7} values (Table II). Furthermore, in the case of M183H mutant, two distinct cyt c_1 subpopulations with different properties appear to coexist, suggesting that one of them may correspond to a bis-histidine folding intermediate, which is trapped in the absence of the native methionine ligand. bis-Histidine folding intermediates have been observed in the case of horse heart cyt *c* (Yeh *et al.*, 1998; Xu *et al.*, 1998). The findings established that in *R. capsulatus*, the sixth axial ligand is not essential either for the attachment of the heme group to cyt c_1 or for the assembly of this subunit into the bc_1 complex. Yet, it appears that, besides affecting the E_m value of cyt c_1, it may also be important for its proper folding. Future characterizations of purified cyt c_1 subunits should further establish the identity of the axial ligands in these mutants and shed light into cyt c_1 folding pathway.

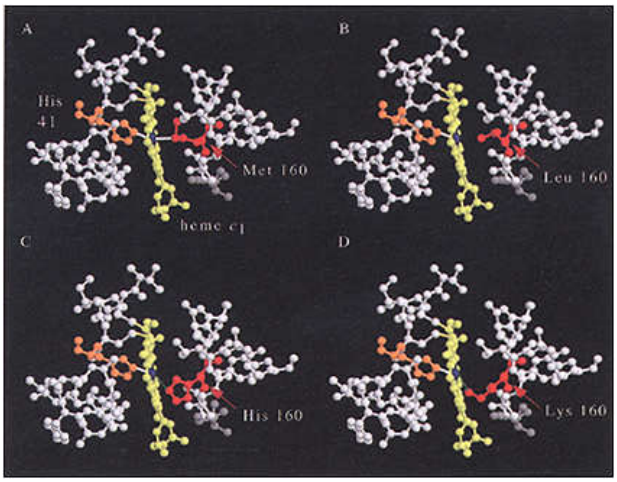

Fig. 2. Heme binding region of cyt c_1 subunit of the bc_1 complex. Hypothetical three-dimensional structures of cyt c_1 mutants using the coordinates of the bovine heart mitochondrial bc_1 complex (Iwata *et al.*, 1998). Panels A, B, C, and D depict the wild-type (M160), and M160L, M160H, and M160K cyt c_1 mutants corresponding to *R. capsulatus* wild-type (M183) and M183L, M183H, and M183K mutants, respectively. The residues surrounding heme (in yellow) are shown in gray, the fifth ligand histidine 41 (histidine 38 in *R. capsulatus*) in orange, and the different amino acid residues at position 160 (position 183 in *R. capsulatus*) occupying the sixth ligand position, in red. The coordination between His41 or Met160 and the iron atom of heme is in white and the possible coordination between the histidine (in M183H) or lysine (in M183K) and the iron atom is shown in green.

Table II. Properties of *Rhodobacter capsulatus* cyt c_1 Sixth Axial Ligand M183 Mutants

Strain	Phenotype[a]	Properties of cyt c_1 heme[b] E_{m7} (mV)	λ_{max} (nm)	References
Wild type	Ps^+	310–340	551–552	Gray *et al.*, 1992
M183H	Ps^2	30–50 and ' 2140	552–554	Darrouzet *et al.* 1999
M183K	Ps^2	60–80	548–549	Darrouzet *et al.* 1999
M183L	Ps^2	274	551	Gray *et al.*, 1992

[a] Ps^+ and Ps^2 indicate the ability and inability, respectively, to grow photosynthetically on MPYE-enriched medium at 358C.
[b] Properties of cyt c_1 heme group in chromatophore membranes and purified bc_1 complexes.

RIESKE Fe–S PROTEIN SUBUNIT

The Rieske Fe–S protein subunit is also anchored to the membrane by a single membrane-spanning helix, which, in this case, is located at the N-terminus of the polypeptide chain (Van Doren *et al.*, 1993b). The C-terminal end of this subunit bears a high-potential [2Fe–2S] cluster, which is detectable in its reduced state by EPR spectroscopy. The EPR signature of this cluster is very sensitive to changes in its environment and, hence, it has been widely used to monitor the interactions of Q/QH_2 and inhibitors with the Q_o site (Ohnishi *et al.*, 1988; Ding *et al.*, 1992, 1995a,b; Sharp *et al.*, 1998). Earlier biophysical analyses have predicted a coordination of the [2Fe–2S] cluster by two nitrogen and two sulfur atoms (Gurbiel *et al.*, 1991; Britt *et al.*, 1991). Sequence alignment revealed the presence of two conserved hexapeptide sequences, called box I (C_{133}THLGC_{138}) and box II (C_{153}PCHGS_{158}) (*R. capsulatus* numbering) at the C-terminal region of the FeS protein subunit. Site-directed mutagenesis of the two cysteine (C133 and C153) and two histidine residues yielded nonfunctional bc_1 complexes with undetectable FeS apoprotein or [2Fe–2S] cluster (Davidson *et al.*, 1992a; Van Doren *et al.*, 1993a), while substitution of the remaining cysteine (C138 and C155) residues yielded mutants with trace amounts of apoproteins containing perturbed [2Fe–2S] clusters (Davidson *et al.*, 1992a; Ohnishi *et al.*, 1994). These findings inferred that C133, H135, C153, and H156 were the cluster ligands and that C138 and C155 were required for the stability and assembly of the cluster, probably via the formation of an intramolecular disulfide bridge. These assignments have now been consolidated by the 3-D structure of the soluble domain of the Rieske Fe–S protein (Iwata *et al.*, 1996), and that of the bc_1 complex (Xia *et al.*, 1997; Zhang *et al.*, 1998; Iwata *et al.*, 1998).

The role of the nonliganding amino acid residues in close proximity to the [2Fe–2S] cluster and their interactions with the Q_o site was also studied. The E_{m7} values of the [2Fe–2S] clusters of the FeS protein subunits are high in all the organisms oxidizing ubi-QH_2 or plasto-QH_2 (around 300 mV in *R. capsulatus*) (Davidson *et al.*, 1992a) and a bit lower for those using mena-QH_2 (100 to 165 mV) (Liebl *et al.*, 1992). In all cases, these values are much higher than that of the Rieske-type clusters found in bacterial dioxygenases (E_m values ranging from −155 to 0 mV) (Rosche *et al.*, 1995). The basis for this difference is unclear and it has been proposed that electrostatic effects of the residues surrounding the metal cluster and the presence of a hydrogen bond network around it may be important factors (Riedel *et al.*, 1995). Recent work performed using *Paracoccus denitrificans* bc_1 complex indicated that mutation of Ser157 and Tyr159 (corresponding to Ser158 and Tyr160 in *R. capsulatus*) proposed to be hydrogen bonded with one of the sulfur atoms of the cluster and with the Cys132 (Cys133 in *R. capsulatus* numbering) sulfur atom, respectively, yielded Rieske Fe–S proteins with E_{m6} values decreased by 100 and 40 mV, respectively (Schroter *et al.*, 1998). Similar results have also been obtained with the yeast protein (Denke *et al.*, 1998).

Concerning the role of amino acid residues of the conserved boxes, earlier studies using yeast had shown that Rieske Fe–S protein mutants at positions corresponding to 137, 140, and 154 of that of *R. capsulatus* exhibited diminished electron transfer activity, decreased E_m values, and partial loss of the [2Fe–2S] cluster and apoprotein (Beckman *et al.*, 1989; Gatti *et al.*, 1989). Similarly, the *R. sphaeroides* Rieske Fe–S protein mutant G137D also yielded a poorly functional bc_1 complex with a decreased Q_o site turnover rate (Van Doren *et al.*, 1993a). These findings suggested that these positions might be important for the conformation of the peptide loops around the [2Fe–2S] cluster and, hence, the stability of the metal cluster. A more systematic study performed using two sets of mutants at position Thr134 and Leu136 of *R. capsulatus* Fe-S protein subunit confirmed the influence of these amino acid residues on the properties of the [2Fe–2S] cluster and on its interactions with Q/QH_2 at the Q_o site (Liebl *et al.*, 1997) (Fig. 3). The mutations at position 134 mainly affect the E_m values and oxygen sensitivity of the [2Fe–2S] cluster, while those at position 136, in addition, impair the activity of the Q_o site and the interactions of the Fe–S protein subunit with Q/QH_2 and stigmatellin (Table III). Very interestingly, the nonfunctional mutants at position 136 were found to revert with a second mutation located in the N-terminal portion of the Rieske Fe–S protein, at positions V44 and A46 (Brasseur *et al.*, 1997) (Fig. 3). These second-site revertants located 40 A away from the [2Fe–2S] provided the first indication that the flexible N-terminal region of the Rieske Fe–S protein was also implicated in Q_o site catalysis and controlled the E_m value of its metal cluster (Table IV).

Further investigations of the N-terminal domain of the Fe–S protein subunit were undertaken in the light of its plausible movement during Q_o site catalysis. Various mutations changing the composition, length,

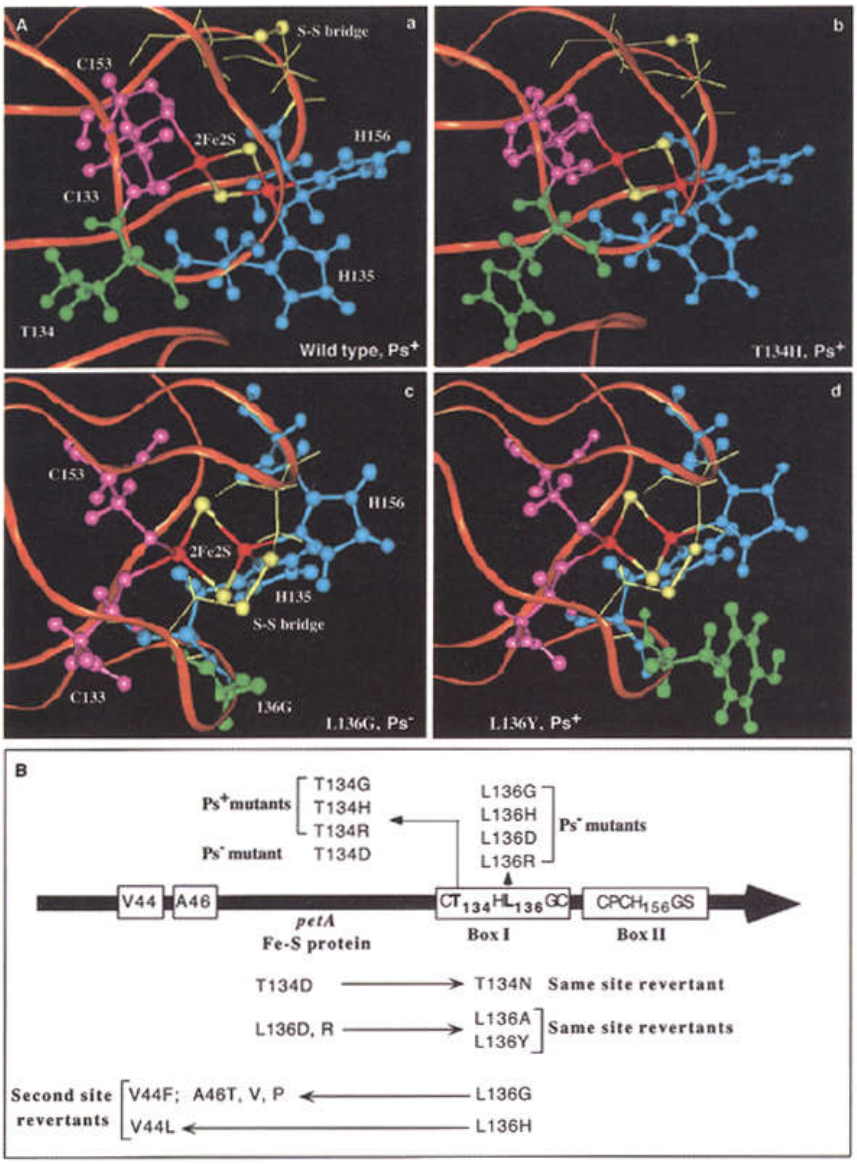

Fig. 3. (A) Visualization of the 3-D conformation of the cluster-binding domain in various *R. capsulatus* Rieske Fe–S proteins. The atomic coordinates of the bovine soluble Rieske FeS protein (Iwata *et al.*, 1996) were used and the wild type (a), the Ps^2 mutants T134H (b), L136G (c), and the Ps^+ revertant L136Y (d) are shown. Iron and sulfur atoms of the [2Fe–2S] cluster are colored in red and yellow, respectively. The two histidine ligands corresponding to His135 and His156 (*R. capsulatus* numbering) are shown in blue, while the Cys133 and Cys153 ligands are in pink and the Cys138 and Cys155 residues forming a disulfide bridge are in yellow. The green residue highlights position 134 or 136 (140 or 142, respectively, in the bovine protein) where the mutations are displayed. Note that the T134 and L136 mutants are shown from different perspectives in order to better visualize the corresponding substitutions. (B) *Rhodobacter capsulatus* Rieske Fe–S protein mutants and their revertants. The conserved Box I and II sequences containing the four ligands of the [2Fe–2S] cluster (C133, H135, C153, and H156) as well as the two cysteine residues (C138 and C155) forming a disulfide bridge, are shown. The same-site revertants at position 134 or 136 in the C-terminal portion and the second-site suppressor mutations at positions 44 and 46 at the N-terminal portion of the Rieske Fe–S protein are indicated.

Table III. Characteristics of *Rhodobacter capsulatus* Rieske Fe–S Protein Mutants T134 and L136

Strain	Phenotype/ dt (min)[a]	bc_1 complex activity[b] (%)	[2Fe–2S] E_{m7}[c] (mV)	Response to Q/QH_2[d]	Response to Stig[e]
Wild type	Ps^+ / 170	100	310	+	+
bc_1^-	Ps^-/na	< 1	na	na	
T134R	Ps^+ / 170	24	260	+	+
T134H	Ps^+ / 240	10	230	+	+
T134G	Ps^+ / 320	10	210	+	+
T134D	Ps^- / na	2	nd	nd	nd
T134N	Ps^+ / 185	16	nd	nd	nd
L136R	Ps^- / na	5	278	−	−
L136H	Ps^- / na	4	289	−	+/−
L136G	Ps^- / na	4	196	−	+/−
L136D	Ps^- / na	2	235	−	+/−

[a] Ps^+ and Ps^- indicate photosynthetic competence and incompetence, respectively, and doubling times (dt) are for photosynthetic growth in MPYE-enriched medium; na, not applicable.
[b] Steady-state bc_1 complex activity was determined by measuring the DBH_2 cyt *c* reductase activity, and expressed as a percentage of the wild-type activity.
[c] The E_{m7} values were obtained after fitting the amplitude of the EPR g_y signal during potentiometric titration of the Rieske [2Fe–2S] cluster; nd, not determined.
[d] Q/QH_2: + or − indicates that the mutants are able or unable, respectively, to detect the change in the reduced state of the Q_{pool} as reflected by the shape of the EPR g_x signal of the [2Fe–2S] cluster.
[e] Stig: + or − indicates that the mutants are able or unable, respectively, to respond to stigmatellin, and +/− indicates that they respond to it differently than the wild-type, as revealed by the shape of the EPR g_x signal of their [2Fe–2S] clusters.

Table IV. Characteristics of *Rhodobacter capsulatus* Rieske Fe–S Protein Ps^+ Revertants of L136 mutants

Strain	dt (min)[a]	Electron transfer $QH^2 \rightarrow$ cyt c^b (%)	[2Fe–2S] E_{m7}[c] (mV)	EPR g_x values[d] Q	QH_2	Stig
Wild type	170	100	312	1.799	1.782	1.778
L136H/V44L	190	nd	245	1.748	1.743	1.807
L136G/V44F	240	16	245	1.76 (broad)	1.77 (broad)	1.74 (broad)
L136G/A46T	215	25	248	1.758	1.756	1.723
L136G/A46V	215	nd	nd	nd	nd	nd
L136G/A46P	205	nd	nd	nd	nd	nd

[a] Doubling times (dt) are for photosynthetic growth in MPYE-enriched medium.
[b] QH_2 to cyt *c* electron-transfer rates were determined by recording cyt *c* rereduction kinetics at 550–540 nm and fitting them to single exponential equation. They are expressed as a percentage of that of the wild type and reflect single-turnover bc_1 complex activity.
[c] The E_{m7} values were obtained after fitting the amplitude of the EPR g_y signal during potentiometric titration of the Rieske [2Fe–2S] cluster.
[d] The EPR g_x values correspond to the center of the trough at 200 mV (Q), 0 mV (QH_2), and 200 mV + 40 μM stigmatellin (Stig); nd, not determined.

and rigidity of its flexible N-terminal "neck" region were obtained (Darrouzet *et al.*, 1998, in press; Darrouzet *et al.*, manuscripts in preparation) (Fig. 4). Ongoing analyses reveal that none of the amino acid residues constituting the flexible neck region of the Fe–S protein subunit plays an essential catalytic function per se, since all single substitutions in all positions tested yield almost wild type-like bc_1 complexes. Shortening the length of this region is also well tolerated, but either increasing its length or decreasing its flexibility is deleterious for the function of the bc_1 complex (Table V). Detailed characterization of the properties of these mutants and their revertants should lead to a better definition of the close relationship existing between this flexible neck region of the Fe–S protein subunit and Q_o site catalysis. Similar, and complementary, studies have also been done recently using *R. sphaeroides*, where a loss of function is observed when the rigidity of the neck region is increased by incorporation of either several proline residues or cysteine residues capable of forming a disulfide bond (Tian *et al.*, 1998, 1999).

An independent approach aimed at revealing possible conformational changes at the neck region of the

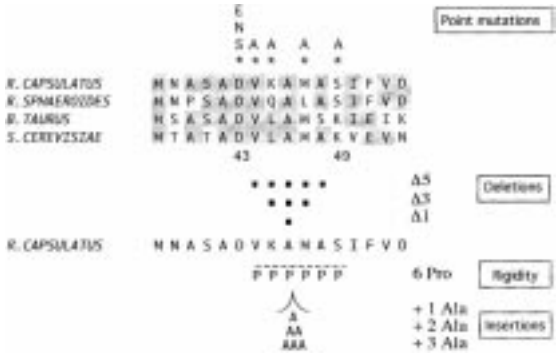

Fig. 4. Various *R. capsulatus* Rieske Fe–S protein neck mutations. The Rieske Fe–S protein sequences from a few selected species aligned with that of *R. capsulatus* between the positions 38 and 53, along with the positions of the different mutations are shown. Stars (*) and squares (■) refer to the point mutations and deletions, respectively. The six proline residues in the mutant "6Pro" replace the six natural amino acid residues of the wild-type protein between the positions 44 and 49. Identical residues are highlighted in gray, single amino acid substitutions are shown above the sequences, and the insertion site of the additional alanine residues is also indicated.

Table V. Characteristics of *Rhodobacter capsulatus* Rieske Fe–S Protein Neck Mutants

Strain	Phenotype[a]	Electron transfer $QH_2 \rightarrow$ cyt c^b(%)	Assembly[c]
Wild Type	Ps^+	100	100
bc_1^-	Ps^-	0	na
D43E, G, H, N, S V44A, L, F K45A, A46T, V M47A, S49A	Ps^+	50–100	45–100
Δ46	Ps^+	50	70
Δ45–47	Ps^+	50	30
Δ44–49	Ps^+	7	20
+ 1 Ala46	Ps slow	35	105
+ 2 Ala46	Ps^-	2	130
+ 3 Ala46	Ps^-	0	140
6 Pro (44–49)	Ps^-	0	50

[a] Ps^+ and Ps^- indicate photosynthetic competence and incompetence, respectively, for photosynthetic growth in MPYE-enriched medium.

[b] QH_2 to cyt *c* electron-transfer rates were determined by recording cyt *c* rereduction kinetics at 550–540 nm and fitting them to a single exponential equation. They are expressed as a percentage of that of the wild type, and reflect single-turnover bc_1 complex activity.

[c] Assembly refers to the stoichiometry of the Fe–S protein subunit to cyt c_1 or cyt *b* subunits as determined by scanning of appropriate SDS-PAGE gels and immunoblots and expressed as a percentage of the wild type; na, not available.

Fe–S protein subunit during Q_o site catalysis, or upon binding of inhibitors like stigmatellin, has made use of thermolysin-mediated controlled proteolysis of the bc_1 complex (Darrouzet *et al.*, 1998, in press). Upon digestion of the bovine mitochondrial bc_1 complex, thermolysin releases a soluble form of the Fe–S protein subunit by proteolytic cleavage at its neck region (Link *et al.*, 1996). This approach was first adapted to purified *R. capsulatus* bc_1 complex and then the effect of various inhibitors on the proteolysis of its Fe–S protein subunit was determined (Fig. 5). Clearly, the presence in the assay mixture of stigmatellin, but not that of antimycin A or myxothiazol, completely blocks the proteolytic cleavage of this subunit at its neck region, inferring that the conformation of this region must be modified under these conditions (Darrouzet *et al.*, 1998, in press; Valkova-Valchanova *et al.*, manuscript in preparation). Such a conformational change has been seen in the mitochondrial bc_1 structure obtained in the presence of stigmatellin (Zhang *et al.*, 1998) (Fig. 1). Thus, it provides a handy tool for monitoring the behavior of the Fe–S protein subunit of mutants that affect the different steps of QH_2 oxidation by the bc_1 complex.

CYTOCHROME *b* SUBUNIT

In earlier studies, various cyt *b* residues affecting Q/QH_2 accessibility and binding, like F144, G152, and G158 (Ding *et al.*, 1995a,b; Tokito and Daldal, 1993; Atta-Asafo-Adjei and Daldal, 1991) or electron transfer reactions, like Y147 (Saribas *et al.*, 1995) at the Q_o site had already been reported (for a review, see Brasseur *et al.*, 1996). More recently, it has become clear that the spatial conformation of heme b_L is also important for Q_o site functions. *Rhodobacter capsulatus* mutations G146A and G146V, which affect one of the four invariant glycine residues of cyt *b*, perturb the conformation of b_L heme as evidenced by its modified EPR g_Z signal and alter substrate accessibility and binding to the Q_o site without disturbing the E_m values of the *b* hemes or the assembly of the bc_1 complex (Saribas *et al.*, 1997). In support of this finding, the extremely close proximity of Gly146 residue (corresponding to Gly131 in bovine cyt *b*) to heme b_L edge was confirmed by the 3-D structure of the mitochondrial bc_1 complex (Xia *et al.*, 1997).

Much less is known about the Q_o site residues involved in subunit interactions that mediate the assembly of the bc_1 complex and the postulated movement of the Fe–S protein subunit during catalysis. Studies of yeast mutants had indicated that the cluster region of the Fe–S protein subunit may interact with cyt *b* in the vicinity of its surface helixes *cd*1 and *cd*2 (Giessler *et al.*, 1994). Serendipitous discovery of *R. capsulatus* cyt *b* mutant T163F, which is unable to assemble the bc_1 complex shed more light on the critical role of these regions in mediating subunit interactions at the Q_o site (Saribas *et al.*, 1998). In particular, analyses of the Ps^+ revertants of T163F have revealed that the loss of the hydroxyl group at position 163 of cyt *b* can be compensated by the gain of either a hydroxyl group at position 182 (Gly to Thr) of cyt *b* or at position 46 (Ala to Thr) of the Fe-S protein subunit or a sulfhydryl group at position 46 (Arg to Cys) of cyt c_1 (Fig. 6). These second-site revertants contained substoichiometric amounts of the Fe–S protein subunit and restored, only partially, the activity of the enzyme (Table VI), as well as the occupancy of the Q_o site as indicated by their EPR g_X signal with the Q_{pool} fully oxidized. Unexpectedly, they also produced, via proteolysis, a soluble form of the Fe–S

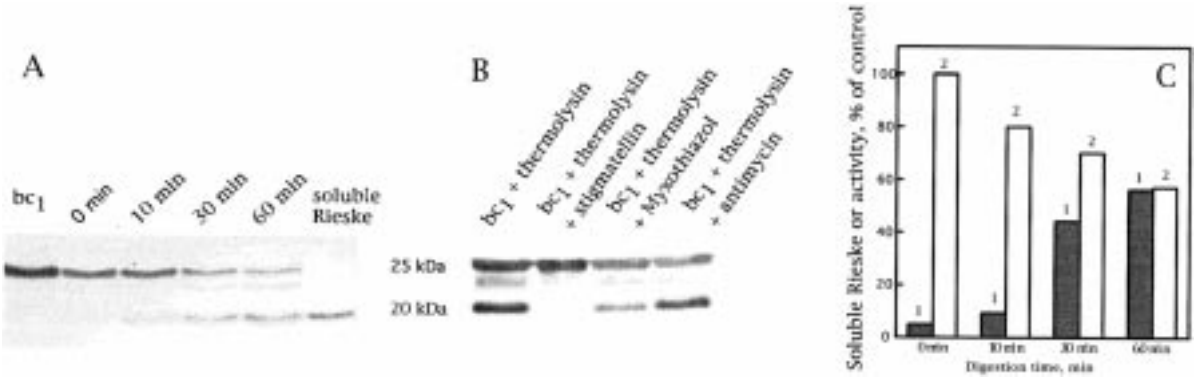

Fig. 5. Thermolysin-mediated proteolysis of purified *R. capsulatus* bc_1 complex. Aliquots were removed at indicated times and analyzed either by immunoblotting using polyclonal antibodies against the Rieske Fe–S protein of *R. capsulatus* (A and B) or assayed for DBH_2 cyt *c* reductase activity. The data are represented as a bar graph in (C): gray bars (1) represent the percentage of soluble Rieske FeS protein and white bars (2) the DBH_2 cyt *c* reductase activity. (B) illustrates the effect of various bc_1 complex inhibitors on thermolysin-mediated proteolysis of the Rieske Fe–S protein. Purified bc_1 complex was incubated for 60 min in the presence of 0.2% (w/v) thermolysin and 20 μ*M* stigmatellin or 10 μ*M* myxothiazol or 20 μ*M* antimycin.

protein subunit missing its first 43 residues, probably because of a conformational change of the flexible neck region of this subunit within the bc_1 complex. Examination of the 3-D structure of the mitochondrial bc_1 complex reveals that the counterparts of G182 (i.e., G167 in bovine) of cyt *b* and A46 (i.e., A70) of the Fe–S protein subunit are located in close proximity to the initial T163 (i.e., T148) position in cyt *b*, whereas the location of R46 (i.e., R28) of cyt c_1 is remarkably far away. This observation raises the possibility that subunit interactions may well go beyond the boundaries of a monomer of the bc_1 complex and involve its dimeric structure.

An important issue currently under investigation is the number of Q/QH_2 molecules at the Q_o site and their interactions with the [2Fe–2S] cluster of the Fe–S protein subunit during catalysis. In this respect, the EPR signature of the Rieske [2Fe–2S] cluster, a highly sensitive probe to monitor changes at the Q_o site, such as the redox state of the Q_{pool}, or occupancy of the site by Q/QH_2 and various inhibitors, was used in combination with stepwise Q extractions from chromatophore membranes. Analyses of the different EPR g_X signals led to the model of "double occupancy" for the Q_o site (Ding *et al.*, 1992, 1995a). The effect of adding ethanol and other water-soluble alcohols with longer side chains to the chromatophores of *R. capsulatus* on the shape of the EPR signal of the Fe–S protein subunit was also analyzed (Sharp *et al.*, 1998). Alcohols uncouple the ability of the [2Fe–2S] cluster to monitor Q_o site occupancy without altering the activity of the bc_1 complex, suggesting that they compete with Q/QH_2 for forming an hydrogen bond with the NεH of the liganding histidines and that this effect is apparently not inhibitory for Q_o site functions. More recently, these studies were further pursued using judiciously chosen weak Q_o site inhibitors, like diphenylamine (DPA) or MOA-stilbene. At micromolar concentrations, DPA inhibits cyt c_1 rereduction without interfering with the interactions of the [2Fe–2S] cluster with Q/QH_2 at the Q_o site, thus behaving like a noncompetitive inhibitor of QH_2 oxidation (Sharp *et al.*, 1999). However, at millimolar concentrations DPA also competes with Q/QH_2 of lower affinity (Q_{ow}) at the Q_o site and yields an EPR g_x signal characteristic of one Q/QH_2 at the site.

ASSEMBLY OF THE DIFFERENT SUBUNITS AND ENGINEERING OF NOVEL bc_1 COMPLEXES

It is known that bacterial mutants devoid of the Fe–S protein subunit, unlike those lacking cyt c_1 still contain in their chromatophore membranes a subcomplex formed of cyt *b* and cyt c_1 (called b–c_1 subcomplex) (Davidson *et al.*, 1992b). Recently large amounts of *R. capsulatus* b–c_1 subcomplex was purified to homogeneity and characterized (Valkova-Valchanova *et al.*, 1998). Its properties are very similar to those of a wild-type bc_1 complex in many aspects, including the integrity of its Q_i site, except that indeed its Q_o site is nonfunctional and its heme b_L is perturbed. Its inactive Q_o site can be readily reactivated for the cyt *c*

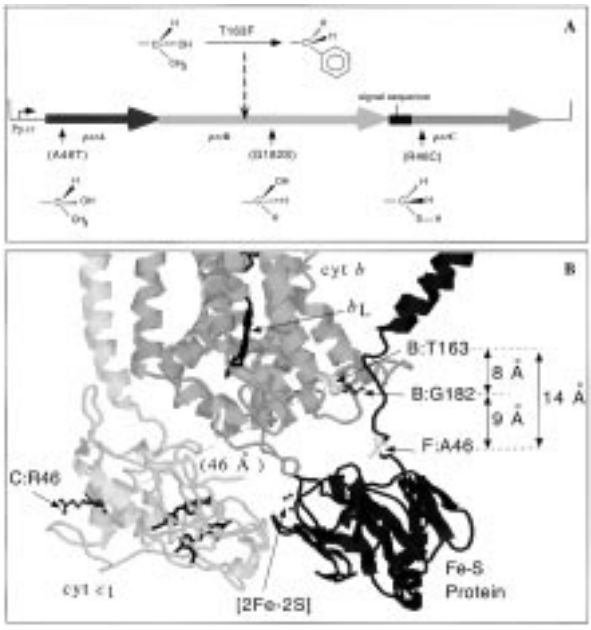

Fig. 6. (A) *Rhodobacter capsulatus* cyt *b* T163F mutation and its second-site suppressors. Genetic locations of cyt *b* (*pet*B) T163F mutation and its second-site suppressors A46T in the Fe–S subunit (*pet*A), G182S in cyt *b*, and R46C in cyt c_1 (*pet*C) subunits are shown along with the chemical structures of the modified amino acid side chains in each case. (B) Visualization on the mitochondria bc_1 complex structure of the intra- and intergenic suppressors of cyt *b* T163F mutation. The figure depicts the region surrounding position T163 of cyt *b* (T148 in the mitochondrial bc_1 complex) with positions G182 (cyt *b* subunit) and A46 (Fe–S protein subunit), corresponding to G167 and A70, respectively, in bovine heart mitochondrial bc_1 complex. It also shows the distant position R64 in cyt c_1 subunit (R28 in the mitochondrial structure). The picture is generated using the atomic coordinates from the chicken bc_1 complex and the closest distances between various amino acid residues are measured using RasMol 2.6-ucb1.0.

reductase activity by addition of purified Fe–S protein subunit with an intact membrane anchor (Fig. 7). A soluble derivative of the Fe–S protein subunit lacking the N-terminal anchor domain is unable to reactivate the purified b–c_1 subcomplex, although it can still bind to the Q_o site in the presence of stigmatellin. These studies revealed that the Fe–S protein subunit interacts with two distinct regions of the bc_1 complex and is able to reassemble per se into a preassembled b–c_1 subcomplex provided that its N-terminal membrane anchoring domain is present. Moreover, shortening the length of the neck region of the Fe–S protein subunit leads to its poor assembly into the bc_1 complex *in vivo*, further supporting its critical role for both the assembly and the function of the bc_1 complex (Darrouzet *et al.*, 1998, in press; Darrouzet *et al.*, manuscript in preparation) (Table V).

Table VI. Ps^+ Revertants of *Rhodobacter capsulatus* cyt *b* TI63F Mutants

Strain	Phenotype dt in min)[a]	bc_1 complex activity[b] (%)	Assembly[c] (%)	Electron transfer $QH_2 \rightarrow$ cyt c[d] (%)
Wild type	Ps^+(120)	100[b]	100	100
B:T163F	Ps^-	0	0	0
(B:T163F + B:G182S)	Ps^+(170)	3	30	23
(B:T163F + C:R46C)	Ps^+(210)	3	40	19
(B:T163F + F:A46T)	Ps^+(150)	21	55	77
B:G182S	Ps^+(140)	20	nd	45
C:R46C	Ps^+(190)	32	nd	88
F:A46T	Ps^+(140)	92	nd	65

[a] Ps^+ and Ps^- indicate photosynthetic competence or incompetence, respectively, and the doubling times are for photosynthetic growth in MPYE-enriched medium.
[b] Steady-state bc_1 complex activity was determined by measuring the DBH_2 cyt *c* reductase activity expressed as a percentage of the wild-type activity.
[c] Assembly refers to the stoichiometry of the Fe–S protein subunit in respect to cyt c_1 subunit as determined by scanning of appropriate SDS–PAGE gels and expressed as percentage of the wild type.
[d] QH_2 to cyt *c* electron-transfer rates were determined by recording cyt *c* rereduction kinetics at 550–540 nm and fitting them to a single exponential equation. They are expressed as a percentage of the wild type and reflect single-turnover bc_1 complex activity.

The b_6f complex, which is a functional counterpart of the bc_1 complex in chloroplasts and cyanobacteria, contains four major subunits. Among them, cyt b_6 and subunit IV(su IV), which have four and three membrane-spanning helixes, respectively, show about 60% similarity to the N- and C-terminal portions of cyt *b*, respectively. This pronounced similarity has previously led to the proposal that cyt b_6 and su IV may be evolved from the splitting of cyt *b* (Widger *et al.*, 1984). With a sophisticated genetic system and a 3-D structure at hand, rationale engineering of the bc_1 complex into variants similar to its counterparts found in other organisms was attempted. A novel kind of bc_1 complex, called b_6c_1 complex, was created using *R. capsulatus* by splitting genetically *petB* gene into two cistrons to mimic the b_6f complex (Mandaci *et al.*, 1998, in press; Saribas *et al.*, 1999). This effort yielded an active enzyme able to support the Ps growth of *R. capsulatus* and showed clearly that cyt *b* helixes contained enough structural information to reassemble into a functional enzyme *in vivo*. The new created b_6c_1

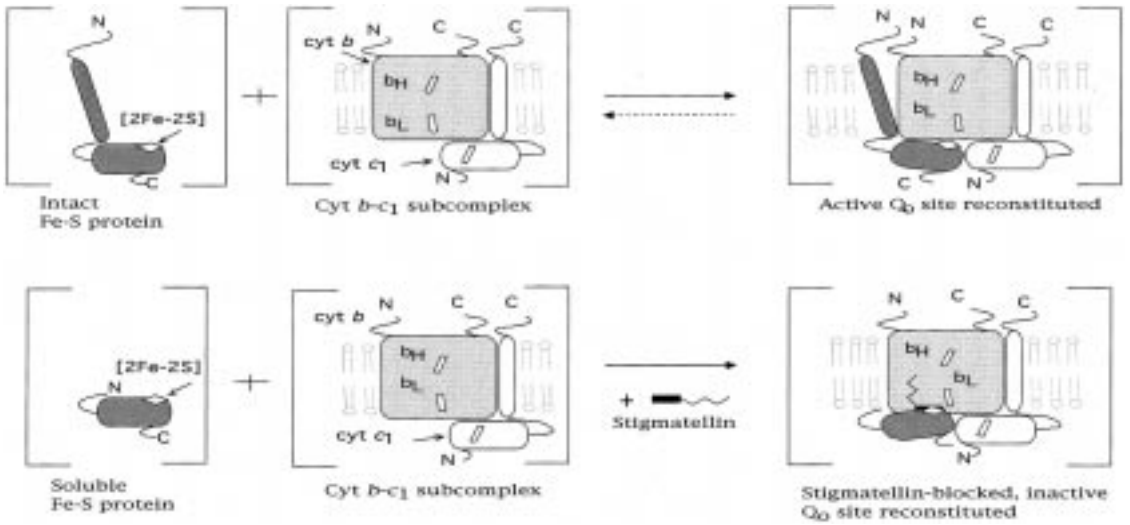

Fig. 7. Reconstitution *in vitro* of bc_1 complexes. Schematic representation of the reconstitution *in vitro* of purified *R. capsulatus* b–c_1 subcomplex with purified intact Fe–S protein subunit, or with a soluble derivative of it lacking its first 43 N-terminal amino acid residues containing its membrane-anchor domain, in the presence of stigmatellin.

complex retained the overall characteristics of the bc_1 complex, with the exception that the optical spectrum of its heme b_L was converted to a form resembling that seen with the b_6f complexes (Fig. 8). Thus, splitting a long cyt *b* into two smaller polypeptides does not account for the other differences observed between the bc_1 and b_6f complexes. Similar and complementary results have also been obtained using *R. sphaeroides* bc_1 complex (Kuras *et al.*, 1998). These initial attempts now pave the road toward the creation of novel *bc* complexes, hopefully with interesting properties, via structure-based rationale engineering approaches *in vivo*.

SUMMARY AND FUTURE ISSUES

During the last few years, research on the bc_1 complex has been very active and exciting, and tremendous progress has been achieved. Yet, many unanswered questions and new issues extending from its mechanism of function to its assembly and biogenesis still stand out. The resolution of the 3-D structure of this important energy-transducing membrane enzyme has added a wealth of information to the already existing sophisticated body of knowledge and further sharpened the available tools for studying the bc_1 complex in greater detail. The structural data has confirmed and consolidated earlier findings, added atomic-scale precision to our knowledge, and raised new and challenging issues on the mechanism of function and dynamic interactions between the subunits of this complex.

Concerning the mechanism of function, bifurcation of the electrons at the Q_o site via a plausible movement of the Fe–S protein subunit within the bc_1 complex during catalysis is a striking intellectual step forward. However, whether this movement is random or is somehow triggered at the molecular level, and if so how, is completely unknown. This crucial issue deserves further investigations aimed at directly monitoring the mobility of the head domain of the Fe–S protein subunit using both solid state as well as unfrozen and non crystallin forms of the bc_1 complex. In this respect, along with the proteolysis experiments, EPR-based studies using oriented samples have already been initiated, and hopefully will provide otherwise unattainable information (Brugna *et al.*, 1998; T. Ohnishi, personal communication). Still today, most of the molecular events during Q_o site catalysis, from the nature and type of the occupants to the path of the electrons and protons, form a black box. The recently described binding of dicyclohexylcarbodiimide to Asp187 in *R. sphaeroides* may be a lead to such a proton pathway (Wang *et al.*, 1998). Moreover, the communication paths between the Q_i and Q_o sites both within a monomer, and between the monomers of a dimer, are totally obscure and deserve detailed structural and functional studies. Undoubtedly, better crystals and better refined structures, hopefully also from

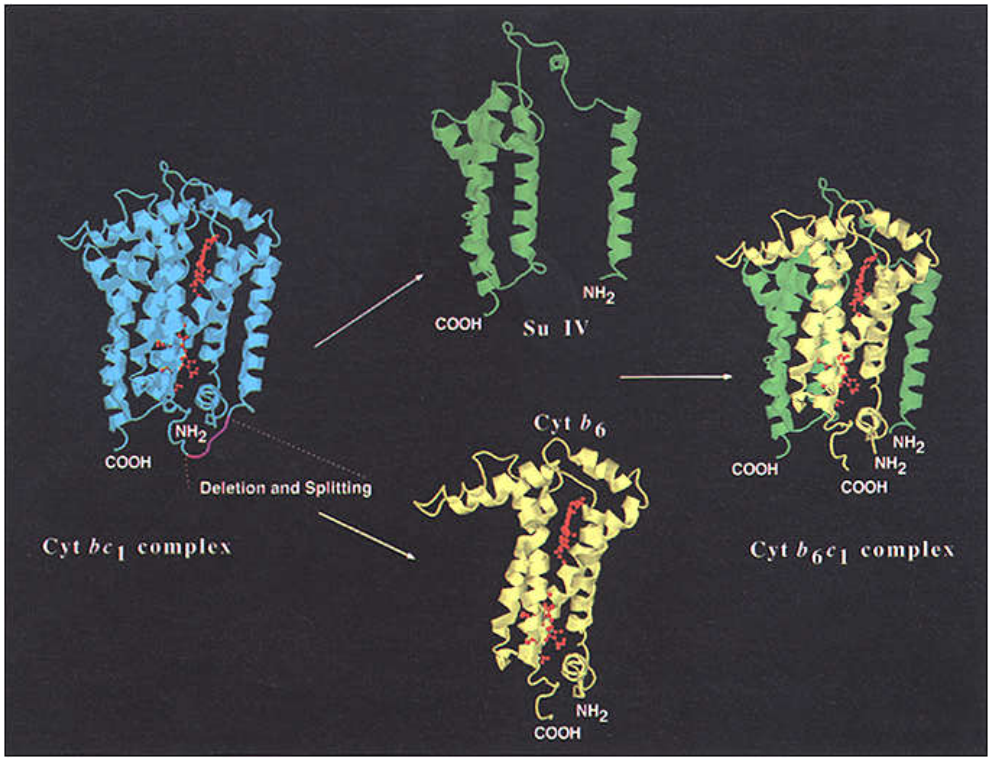

Fig. 8. A 3-D depiction of cyt b_6 and su IV subunits of the cyt b_6c_1 complex. Atomic coordinates from the chicken bc_1 complex (Zhang *et al.*, 1998) were used and the model is built on the hypothesis that the newly created cyt b_6 and su IV subunits reassemble as in the native cyt *b*. The region of cyt *b*, where splitting took place, was modified using homology between the chicken and *R. capsulatus* cyt *b* subunits.

organisms that are amenable to facile genetic approaches, will become available soon. Concerning the interactions between the different subunits, more remains to be discovered especially in the light of their dynamic behaviours during catalysis. The complex interplays between the neck region of the Fe–S protein subunit, the disulfide-bridged peptide loops around the [2Fe–2S] cluster, and the *cd* and ***ef*** loops of cyt *b* are only now emerging, and need to be defined at the atomic scale.

Concerning the assembly and biogenesis of the subunits of the bc_1 complex, while a glimpse about the rules governing the association of the Fe–S protein subunit with a preassembled b–c_1 subcomplex, or the formation *in vivo* of a b_6c_1-like functional complex is now available, we are still far away from correlating rigorously the similarities and differences between various related complexes to unify the different members of the cyt *bc* complex superfamily. Recently encountered bc_1 complex variants from Gram-positive bacillae, somewhat reminiscent of the b_6f complexes (Yu *et al.*, 1995; Yu and Le Brun, 1998; Sone *et al.*, 1996; Xiong *et al.*, 1998), exhibit marvellous evolutionary rearrangements of their subunits. They also provide an obvious guiding light for the engineering of novel *bc* complexes with specifically designed properties.

In short, the issues briefly mentioned above and many others, deserve further investigations if we were to understand how a bc_1 complex works as a redox-driven pump and ultimately use this understanding to design future devices mimicking efficiently Q_o site catalysis. Although such a road currently seems to be tortuous and distant, yet it is clear that bacterial models, in particular that from *Rhodobacter* species, will continue to be of choice for multidisciplinary studies on the structure, function, regulation, and biogenesis of the *bc* complexes.

ACKNOWLEDGMENT

This work was supported by NIH Grant GM 38237 to F. D.

REFERENCES

Atta-Asafo-Adjei, E., and Daldal, F. (1999). *Proc. Natl. Acad. Sci. U.S.A* **88**, 492–496.

Beckman, J. D., Ljungdahl, P. O., and Trumpower, B. L. (1989). *J. Biol. Chem.* **264**, 3713–3722.

Brandt, U., and Trumpower, B. (1994). *Crit. Rev. Biochem.. Mol. Biol.* **29**, 165–197.

Brasseur, G., Saribas, A., and Daldal, F. (1996). *Biochim. Biophys. Acta* **1275**, 61–69.

Brasseur, G., Sled, V., Liebl, U., Ohnishi, T., and Daldal, F. (1997). *Biochemistry* **36**, 11685–11696.

Britt, R. D., Sauer, K., Klein, M. P., Knaff, D. B., Kraiuciunas, A., Yu, C.-A., Yu, L., and Malkin, R. (1991). *Biochemistry* **30**, 1892–1901.

Brugna, M., Albouy, D., and Nitschke, W. (1998). *J. Bacteriol.* **180**, 3719–3723.

Cramer, W., Soriano, G., Ponomarev, M., Huang, D., Zhang, H., Martinez, S., and Smith, J. (1996). *Annu. Rev. Plant Physiol.* **47**, 477–508.

Crofts, A. R., Meinhardt, S. W., Jones, K. R., and Snozzi, M. (1983). *Biochim. Biophys. Acta* **723**, 202–218.

Daldal, F., Davidson, E., and Cheng, S. (1987). *J. Mol. Biol.* **195**, 1–12.

Darrouzet, E., Valkova-Valchanova, M., and Daldal, F. (1998). *Proc. XIth Cong. Photosynthesis*, in press.

Darrouzet, E., Mandaci, S., Li, J., Qin, H., Knaff, D. B., and Daldal, F., (1999) *Biochemistry* **38**, 7908–7917.

Darrouzet, E., Valkova-Valchanova, M., and Daldal, F., manuscript in preparation.

Davidson, E., Ohnishi, T., Atta-Asafo-Adjei, E., and Daldal, F. (1992a). *Biochemistry* **31**, 3342–3351.

Davidson, E., Ohnishi, T., Tokito, M. K., and Daldal, F. (1992b). *Biochemistry* **31**, 3351–3358.

Denke, E., Merbitz-Zahradnik, T., Hatzfeld, O. M., Snyder, C. H., Link, T. A., and Trumpower, B. L. (1998). *J. Biol. Chem.* **273**, 9085–9093.

Ding, H., Robertson, D. E., Daldal, F., and Dutton, P. L. (1992). *Biochemistry* **31**, 3144–3158.

Ding, H., Moser, C., Robertson, D., Tokito, M., Daldal, F., and Dutton, P. (1995a). *Biochemistry* **34**, 15979–15996.

Ding, H., Daldal, F., and Dutton, P. L. (1995b). *Biochemistry* **34**, 15997–16003.

Finnegan, M. G., Knaff, D. B., Qin, H., Gray, K. A., Daldal, F., Yu, L., Yu, C.-A., Kleis-San Francisco, S., and Johnson, M. K. (1996). *Biochim. Biophys. Acta* **1274**, 9–20.

Gao, F., Qin, H., Knaff, D. B., Zhang, L., Yu, L., Yu, C. A., Gray, K. A., Daldal, F., and Ondrias, M. R. (1999). *Biochim. Biophys. Acta* **1430**, 203–213.

Gatti, D. L., Meinhardt, S. W., Ohnishi, T., and Tzagoloff, A. (1989). *J. Mol. Biol.* **205**, 421–435.

Gennis, R. B., Barquera, B., Hacker, B., Van, D. S. R., Arnaud, S., Crofts, A. R., Davidson, E., Gray, K. A., and Daldal, F. (1993). *J. Bioenerg. Biomembr.* **25**, 195–209.

Giessler, A., Geier, B. M., di Rago, J.-P., Slonimski, P. P., and von Jagow, G. (1994). *Eur. J. Biochem.* **222**, 147–154.

Gray, K. A., and Daldal, F. (1995). In *Anoxygenic Photosynthetic Bacteria* (Blankenship, R. E, Madigan, M. T., and Bauer, C., eds.), Kluwer Academic Publishers, Dordrecht, The Netherlands, pp. 747–774.

Gray, K. A., Davidson, E., and Daldal, F. (1992). *Biochemistry* **31**, 11864–11873.

Gray, K. A., Dutton, P. L., and Daldal, F. (1994). *Biochemistry* **33**, 723–733.

Gurbiel, R. J., Ohnishi, T., Robertson, D. E., Daldal, F., and Hoffman, B. M. (1991). *Biochemistry* **30**, 11579–11584.

Hacker, B., Barquera, B., Crofts, A. R., and Gennis, R. B. (1993). *Biochemistry* **32**, 4403–4410.

Hacker, B., Barquera, B., Gennis, R. B., and Crofts, A. R. (1994). *Biochemistry* **33**, 13022–13031.

Iwata, S., Saynovits, M., Link, T. A., and Michel, H. (1996). *Structure* **4**, 567–579.

Iwata, S., Lee, J. W., Okada, K., Lee, J. K., Iwata, M., Rasmussen, B., Link, T. A., Ramaswamy, S., and Jap, B. K. (1998). *Science* **281**, 64–71.

Kim, H., Xia, D., Yu, C.-A., Xia, J.-Z., Kachurin, A. M., Zhang, L., Yu, L., and Deisenhofer, J. (1998). *Proc. Natl. Acad. Sci. U.S.* **95**, 8026–8033.

Knaff, D. B. (1993). *Photosyn. Res.* **35**, 117–133.

Konishi, K., Van Doren, S. R., Kramer, D. M., Crofts, A. R., and Gennis, R. B. (1991). *J. Biol. Chem.* **266**, 14270–14276.

Kuras, R., Guergova-Kuras, M., and A. R. Crofts. (1998). *Biochemistry* **37**, 16280–16288.

Liebl, U., Pezennec, S., Riedel, A., Kellner, E., and Nitschke, W. (1992). *J. Biol. Chem.* **267**, 14068–14072.

Liebl, U., Sled, V., Brasseur, G., Ohnishi, T., and Daldal, F. (1997). *Biochemistry* **36**, 11675–11684.

Link, T. A., Saynovits, M., Assman, C., Iwata, S., Ohnishi, T., and von Jagow, G. (1996). *Eur. J. Biochem.* **237**, 685–691.

Lou, B.-S., Hobbs, J. D., Chen, Y.-R., Yu, L., Yu, C.-A., and Ondrias, M. R (1993). *Biochim. Biophys. Acta* **1144**, 403–410.

Mandaci, S., Saribas, A. S., and Daldal, F. (1998). *Proc. XIth Cong. photosynthesis*, in press.

Martinez, S. E., Huang, D., Szczepaniak, A., Cramer, W. A., and Smith, J. L. (1994). *Structure* **2**, 95–105.

Mitchell, P. (1976). *J. Theoret. Biol.* **62**, 327–367.

Ohnishi, T., Brandt, U., and von Jagow, G. (1988). *Eur. J. Biochem.* **176**, 385–389.

Ohnishi, T., Sled, V. D., Rudnitzky, N. I., Meinhardt, S. W., Yagi, T., Hatefi, Y., Link, T., von Jagow, G., Saribas, A. S., and Daldal, F. (1994). *Biochem. Soc. Trans.* **22**, 191–197.

Riedel, A., Fetzner, S., Rampp, M., Lingens, F., Liebl, U., Zimmermann, J.-L., and Nitschke, W. (1995). *J. Biol. Chem.* **270**, 30869–30873.

Rosche, B., Fetzner, S., Lingens, F., Nitschke, W., and Riedel, A. (1995). *Biochim. Biophys. Acta* **1252**, 177–179.

Saribas, A. S., Ding, H., Dutton, P. L., and Daldal, F. (1995). *Biochemistry* **34**, 16004–16012.

Saribas, A. S., Ding, H., Dutton, P. L., and Daldal, F. (1997). *Biochim. Biophys. Acta* **1319**, 99–108.

Saribas, A. S., Valkova-Valchanova, M., Tokito, M. K., Zhang, Z., Berry, E. A., and Daldal, F. (1998). *Biochemistry* **37**, 8105–8114.

Saribas, A. S., Mandaci, S., and Daldal, F., (1999) *J. Bacteriol.* **181**.

Schroter, T., Hatzfeld, O. M., Gemeinhardt, S., Korn, M., Friedrich, T., Ludwig, B., and Link, T. A. (1998). *Eur. J. Biochem.* **255**, 100–106.

Sharp, R. E., Palmitessa, A., Gibney, B. R., Moser, C. C., Daldal, F., and Dutton, P. L. (1998). *FEBS Lett.* **431**, 423–426.

Sharp, R. E., Palmitessa, A., Gibney, B. R., White, J. L., Moser, C. C., Daldal, F., and Dutton, P. L. (1999). *Biochemistry* **38**, 3440–3446.

Simpkin, D., Palmer, G., Devlin, F. J., McKenna, M. C., Jensen, G. M., and Stephens, P. J. (1989). *Biochemistry* **28**, 8033–8039.

Sone, N., Tsuchiya, N., Inoue, M., and Noguchi, S. (1996). *J. Biol. Chem.* **271**, 12457–12462.

Tian, H., Yu, L., Mather, M. W., and Yu, C. -A. (1998). *J. Biol. Chem.* **273**, 27953–27959.

Tian, H., White, S., Yu, L., and Yu, C. -A. (1999). *J. Biol. Chem.* **274**, 7146–7152.

Tokito, M. K., and Daldal, F. (1993). *Mol. Microbiol.* **9**, 965–978.

Valkova-Valchanova, M. B., Saribas, A. S., Gibney, B. R., Dutton, P. L., and Daldal, F. (1998). *Biochemistry* **37**, 16242–16251.

Valkova-Valchanova, M. B., Darrouzet, E., and Daldal, F., manuscript in preparation.

Van Doren, S. R., Gennis, R. B., Barquera, B., and Crofts, A. R. (1993a). *Biochemistry* **32**, 8083–8091.

Van Doren, S. R., Yun, C. -H., Crofts, A. R., and Gennis, R. B. (1993b). *Biochemistry* **32**, 628–636.

Wang, Y., Obungu, V., and Beattie, D. S. (1998). *Arch. Biochem. Biophys.* **352**, 193-198.

Widger, W. R., Cramer, W. A., Herrmann, R. G., and Trebst, A. (1984). *Proc. Natl. Acad. Sci. U. S.* **81**, 674–678.

Xia, D., Yu, C. -A., Kim, H., Xia, J. Z., Kachurin, A. M., Zhang, L., Yu, L., and Deisenhofer, J. (1997). *Science* **277**, 60–66.

Xiong, J., Inoue, K., and Bauer, C. E. (1998). *Proc. Natl. Acad. Sci. U. S.* **95**, 14851–14856.

Yu, J., and Le Brun, N. E. (1998). *J. Biol. Chem.* **273**, 8860–8866.

Yu, J., Hederstedt, L., and Piggot, P. J. (1995). *J. Bacteriol.* **177**, 6751–6760.

Yun, C. H., Crofts, A. R., and Gennis, R. B. (1991). *Biochemistry* **30**, 6747–6754.

Zhang, Z., Huang, L., Shulmeister, V. M., Chi, Y. -I., Kim, K. K., Hung, L. -W., Crofts, A. R., Berry, E. A., and Kim, S. -H. (1998). *Nature* **392**, 677–684.